Applied Catalysis A: General 478 (2014) 38–44

Contents lists available at ScienceDirect

Applied Catalysis A: General

journal homepage: www.elsevier.com/locate/apcata

Palladium nanoparticle's surface structure and morphology effect on the catalytic activity for dry reforming of methane

Ignacio O. Costilla[a,b], Miguel D. Sánchez[b], Carlos E. Gigola[a,*]

[a] Planta Piloto de Ingeniería Química (UNS-CONICET), Camino La Carrindanga Km 7, 8000 Bahía Blanca, Argentina
[b] Instituto de Física del Sur (UNS-CONICET) and Departamento de Física, Universidad Nacional del Sur (UNS), Av. Alem 1253, 8000 Bahía Blanca, Argentina

ARTICLE INFO

Article history:
Received 15 January 2014
Received in revised form 17 March 2014
Accepted 23 March 2014
Available online 31 March 2014

Keywords:
Pd (palladium)
Catalyst preparation
Dry reforming
Particle's morphology
Carbon formation

ABSTRACT

Low loaded Pd/α-Al_2O_3 catalysts (<0.5 wt% Pd) were characterized and tested for CH_4 reforming with CO_2 at 650 °C. The catalysts were prepared by a recharging procedure, using an organometallic precursor, followed by intermediate washing and calcination steps. FTIR spectra of adsorbed CO showed that the Pd surface structure and the particle size were dependent on the number of post-impregnation washing steps. A catalyst sample with a metal dispersion of 33% showing well defined low-index planes (by FTIR) and nearly spherical particles (by TEM) was obtained using two-washing steps. In the reaction, it exhibited a high initial activity followed by a pronounced deactivation due to carbon nanofiber's formation and sintering. TEM analysis of the used catalyst revealed the presence of spherical Pd particles at the end of the fibers that were not attached to the support surface. On the other hand, a high dispersion sample (78%) with a large fraction of Pd atoms with low coordination was obtained by applying three washing steps after impregnation. The presence of small hemispherical particles and larger nearly-flat ones attached to the support were found by TEM. In this case, the catalyst initially showed a very low activity that increased slowly up to a steady value. Although sintering also occurred and the surface structure of the used catalyst resembled the one of the low dispersion catalyst, the amount of carbon formed was quite low. The observed activation under reaction conditions was associated with the slow development of a surface structure that exhibited mainly the (1 0 0) plane favoring methane dissociation. However, the initial interaction of the particles with the support suggested by TEM micrographs seems to remain unaltered despite the particle size increase. Consequently, the process of nanofiber formation and particle separation was inhibited.

1. Introduction

The reforming of CH_4 with CO_2 remains a process of high interest for synthesis gas production due to the availability of large reserves of natural gas with high CO_2 content. Lately, the increasing amounts of landfill gas have added more potential to this process [1]. Synthesis gas derived from dry reforming may be employed for the production of oxoalcohols, dimethyl ether. Liquid fuels or methanol synthesis require proper adjustment of the H_2/CO ratio.

The main disadvantage of dry reforming is the high temperature required to reach acceptable conversion levels (>700 °C). This temperature affects catalyst performance by sintering and carbon deposition. However, laboratory studies have demonstrated that noble metal catalysts, like Pt/ZrO_2, Rh/ZrO_2, Rh/Al_2O_3 and Rh/OMg [2–4], are active and stable for CH_4 reforming with CO_2. Wei and Iglesia [5] have compared the rate of CH_4 reforming with CO_2 as a function of dispersion over Pt, Rh, Ir and Ru, and found that Pt activity is higher and increases with dispersion. This result suggests that surface atoms of small particles are more reactive for CH_4 activation than those on low-index planes.

Less expensive metals, like Ni and Pd, have also been investigated. They are initially very active, but deactivate rather quickly mainly due to carbon buildup. Using Pd/α-Al_2O_3 catalysts of low metal loading (<1%) with a metal dispersion below 20%, we have shown [6] that a high initial activity for CH_4 reforming with CO_2 is followed by marked deactivation. The characterization of the used catalysts demonstrated carbon accumulation and the growth of metal particles [6]. A more detailed study of the carbon material showed the formation of well-defined carbon nanofibers [7].

The carbon buildup on Pd and Ni catalysts could be controlled by the addition of promoters, like Ce or La [6,8]. However, the behavior

* Corresponding author. Tel.: +54 2914861700; fax: +54 2914861600.
E-mail addresses: cgigola@plapiqui.edu.ar, icostilla@plapiqui.edu.ar (C.E. Gigola).

http://dx.doi.org/10.1016/j.apcata.2014.03.030
0926-860X/

of unpromoted supported Pd remains a subject of interest due to its notable high activity for C—H bond activation. It was indeed shown by Yamaguchi and Iglesia [9] that the CH_4 activation rate is much higher on Pd catalysts than on metals like Rh, Pt or Ni. This result was obtained by using samples with a Pd loading of 1.6 wt% and low dispersion (<10%) indicated the participation of large Pd particles with low-index planes in the reaction.

The effect of Pd particle size on the catalytic activity of the mentioned reaction is difficult to investigate due to metal sintering in the presence of H_2 at high temperature, particularly on samples prepared over a low surface area support. In an attempt to remove this limitation, we prepared Pd/α-Al_2O_3 catalysts with a low metal loading (<0.5 wt%) by using a recharging procedure that included successive impregnations and washing steps to avoid or limit the formation of large Pd particles. Fresh and used samples were characterized by FTIR spectroscopy of adsorbed CO, TPR and TEM measurements. The catalytic activity for CH_4 reforming with CO_2 was measured as a function of the time-on-stream at 650 °C by using a stoichiometric feed mixture. The results showed that particles of similar size and surface structure may exhibit a different catalytic behavior. The preparation procedure seems to affect the Pd–support interaction, which in turn influence the particle shape and the carbon formation process.

2. Experimental

2.1. Catalysts preparation

Two Pd/α-Al_2O_3 catalysts were prepared by successive wet impregnations of commercial α-Al_2O_3 using a benzene solution of Pd acetylacetonate (2×10^{-3} g Pd/ml). The support material (Rhone Poulenc, BET area = 10 m^2/g), was crushed and sieved to a particle size of about 0.33 mm corresponding to a 40–50 mesh fraction and calcined at 500 °C before impregnation. The preparation procedure involved the addition of 6.5 ml of Pd acetylacetonate solution to 3 g of α-Al_2O_3. The mixtures were maintained at room temperature for 72 h with occasional stirring. The samples were then filtered, washed two or three times with 5 ml of benzene, dried in flowing nitrogen at 100 °C during 40 min and finally calcined in flowing air at 300 °C for one hour. The introduction of benzene washing steps after each impregnation allowed the removal of the solution retained on the catalyst pores and the fraction of precursor loosely bound to the support surface. In this way, the formation of large particles during drying and calcination was minimized. After calcination, the impregnation–washing procedure was repeated four times to increase the loading. The samples resulting from this recharging procedure were finally reduced in flowing H_2 at 300 °C for 1 h. Using two washings steps after impregnation, sample F with a Pd content of 0.47 wt% was obtained while performing three washing step leaded to sample H with a metal content of 0.37 wt%. Metal weight loadings were determined by atomic absorption spectroscopy.

2.2. Infrared spectra of adsorbed CO

Fresh catalysts were characterized by FTIR of adsorbed CO after each impregnation step. Infrared spectra were recorded on a Fourier transform spectrometer (Nicolet 20 DXB) with a resolution of 4 cm^{-1}. Catalyst samples of 30–50 mg were pressed (5 tons/cm^2) to form 13 mm diameter disks that were placed in a sample holder supported in a cell with CaF_2 windows that permitted *in situ* treatments. The catalysts were reduced at 300 °C for 30 min., evacuated to 10^{-6} Torr and cooled slowly to room temperature under vacuum. A FTIR spectrum under vacuum was obtained and used as a reference. CO (99.99%, Matheson) was introduced at RT at a pressure close to 5 Torr. The IR spectrum of adsorbed CO was then obtained and ratioed with the reference spectrum. The CO/Pd ratio of fresh and used samples was determined using the integrated band intensities of linear (CO_l) and multicoordinated CO (CO_b) species and the proper extinction coefficients; 2.3×10^{-17} and 1.4×10^{-16} cm^{-1}/molec. respectively [10]. The metal dispersion, Pd_s/Pd_t (surface Pd atoms/total Pd atoms), was estimated assuming $H/Pd_s = 1$; $CO_l/Pd_s = 1$ and $CO_b/Pd_s = 0.5$.

2.3. Temperature-programmed reduction

TPR experiments were performed in a conventional apparatus using a Pyrex glass microreactor (i.d., 4 mm; length, 20 cm). Around 0.20 mg of catalyst was first oxidized in a flow of air at 400 °C. The sample was then cooled down to −75 °C in flowing Ar, by means of a liquid nitrogen bath. Then, the carrier gas was switched to 15 cm^3/min of Ar–H_2 mixture gas (5 vol.% H_2) and the bed temperature was increased at a rate of 10 °C/min up to 300 °C. The amount of H_2 consumed or released during reduction was measured with a thermal conductivity detector (TCD) cell. The effluent gas passed through a bed of molecular sieve placed before de TCD in order to remove water formed during TPR experiments. Temperature reduction profiles were measured on fresh and used samples. In order to remove carbon deposits used samples were previously calcined in air at 500 °C.

2.4. TEM measurements

Fresh and used samples of catalyst H were analyzed by transmission electron microscopy (TEM) using a FEI Tecnai F20 supertwin operating at 200 kV (Institute for Materials, Ruhr-Universität Bochum, Germany). Catalyst F was analyzed by TEM using a JEOL 100 CX instrument operated at 100 kV (CCT, Bahía Blanca, Argentina). Pre-reduced samples were suspended in distilled water and placed on holey carbon supported on a copper grid.

2.5. Catalytic activity

Catalytic tests were carried out in a horizontal tubular flow reactor at 650 °C feed with a CH_4/CO_2/Ar (25/25/50) mixture. Catalysts charges of 0.4 g diluted with an equal amount of pure alumina were located in the central section of a one meter long quartz tube (4 mm i.d.) placed in an electric furnace. A total flow rate of 200 cm^3/min, was used. The samples were reduced *in situ* with pure hydrogen at room temperature and heated to the reaction temperature with pure Ar.

Reactants and products were analyzed using two on-line gas chromatographs equipped with TCD cells. One GC used He as a carrier gas and a silica gel column (6′ × 1/8″) held at 90 °C to separate CO_2 from the other components. Another GC used Ar as a carrier gas and a Chromosorb 102 column (14′ × 1/8″) at 303 K to separate H_2, CO and CH_4. A silica gel bed was set after the reactor to remove the water produced by the reverse water gas-shift (RWGS) reaction. The concentration of water in the product stream was calculated from the O_2 material balance equations.

3. Results and discussion

The effect of washing steps after impregnation on the metal loading and the surface structure of the Pd/α-Al_2O_3 catalysts was first investigated by FTIR. Fig. 1 shows the CO adsorption spectra of samples obtained with and without washing steps. Spectrum (a) corresponds to a sample obtained by washing twice after impregnation. The metal loading was 0.1 wt%. In this case, the main band at 2087 cm^{-1} corresponds to CO bonded to Pd atoms with low coordination indicating the presence of small crystallites, while those at

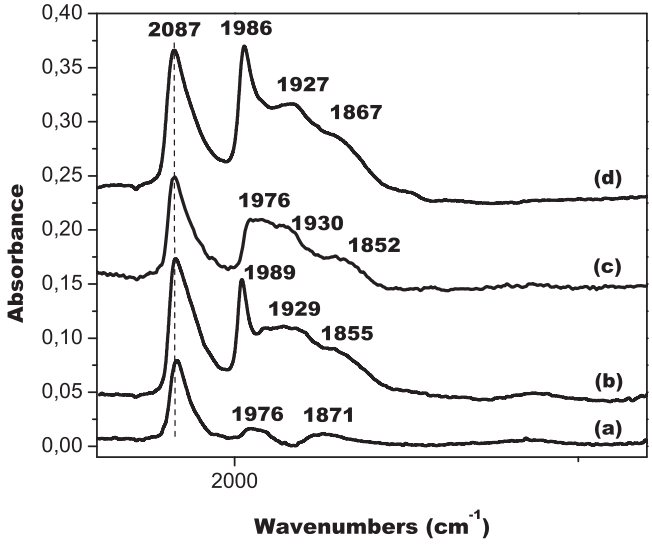

Fig. 1. FTIR spectra of reduced Pd/α-Al_2O_3 catalysts after exposure to 5 Torr of CO at 25 °C. (a) Sample with two washing steps after one impregnation; (b) non washed sample after impregnation; (c) like in (a) plus two additional impregnation–washing cycles; (d) like in (a) with four additional impregnation–washing cycles.

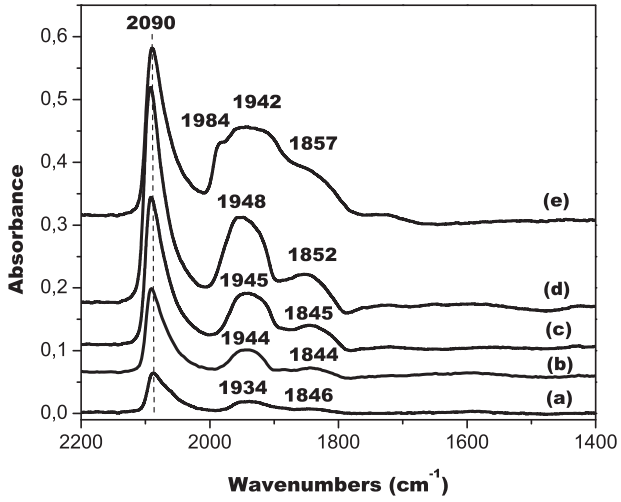

Fig. 2. FTIR spectra of reduced Pd/α-Al_2O_3 catalysts after exposure to 5 Torr of CO at 25 °C. Samples with three washing steps after impregnation. (a) One; (b) two; (c) three; (d) four and (e) five impregnation–washing cycles (sample H).

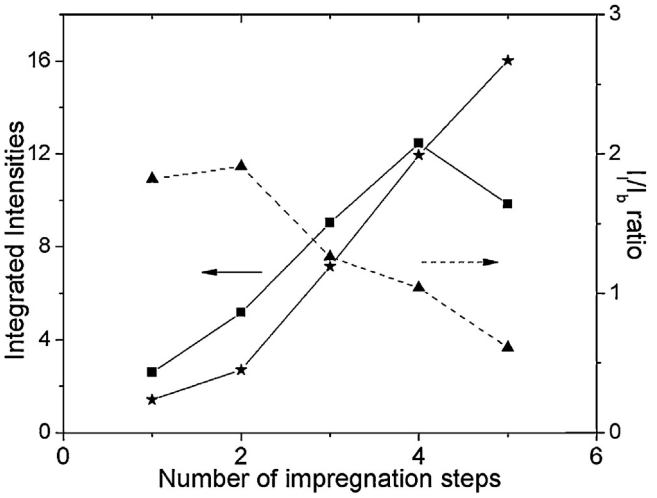

Fig. 3. Effect of the number of impregnation steps on the integrated band intensity of linear (■) (I_l) and multiple coordinated (★) (I_b) CO species and the (▲) (I_l/I_b) ratio. Spectra shown in Fig. 2.

lower frequencies (1976 and 1871 cm^{-1}) are very weak. The CO/Pd ratio for this sample was 0.43 corresponding to a metal dispersion (Pd_s/Pd_t) of 0.47. When the acetylacetonate solution remaining in the pores was not removed, the Pd uptake after impregnation increased to 0.24%. The corresponding spectrum (spectrum (b)) also shows both an intense band due to linear bonded CO at 2087 cm^{-1} and some bands at lower frequencies assigned to multiple coordinated CO. The well-defined band located at 1989 cm^{-1} is commonly assigned to CO adsorption on the Pd(1 0 0) surface plane and the band at 1929 cm^{-1} is due to adsorption on the (1 1 1) face [11]. The calculated CO/Pd ratio for this sample was ≅0.37, which is equivalent to a metal dispersion of 0.46.

In order to obtain samples with a metal content closer to 0.5 wt.%, several impregnations followed by two washing steps were carried out. Fig. 1a, c and d shows the spectra corresponding to samples with one, three and five impregnations. The resulting Pd contents were 0.1, 0.3 and 0.47 wt.% and the CO/Pd ratios were 0.43, 0.27 and 0.26, respectively. The sample with the highest metal content, designated as sample F, has a spectrum similar to that of the sample obtained without washing (spectrum (b) in Fig. 1). Despite the two-fold increase in metal loading, there was a moderate decrease in dispersion; from 0.46 to 0.33. The average particle size based on this value was 3.4 nm (d_p (nm) = 1.12/(Pd_s/Pd_t)). The FTIR spectrum shows well-defined predominant bands at 2087 cm^{-1} and 1986 cm^{-1}, which are commonly assigned to CO on Pd atoms of low coordination, and Pd atoms located on the Pd (1 0 0) face, respectively. It also exhibits two broad features at 1927 cm^{-1} and 1867 cm^{-1} related to CO adsorption on bridge and tree-fold hollow sites.

When a similar preparation procedure was employed, but this time including three washing steps after impregnation, sample H with a metal content of 0.37 wt.% was obtained. After each impregnation–washing cycle, the modification of the CO adsorption spectrum is shown in Fig. 2. In this case the bands due to multiple coordinated CO were located at a lower frequency. Apparently, the number of washing steps influences the precursor anchoring on the support and the formation of Pd crystallites. On spectrum (e) the peak assigned to CO adsorbed on Pd(1 0 0) emerges as a shoulder at 1984 cm^{-1}. Fig. 3 shows the change in the integrated adsorption intensity of linear and multiple coordinated CO as a function of the number of impregnation–washing cycles. The linear band intensity increases continuously and predominates up to the four impregnation step; then, it declines. A comparison of the spectrum of samples F and H clearly shows that the main difference in surface structure is revealed by the intensity of the peak at 1984–1989 cm^{-1}, which is very intense and well defined only in the former sample. Other physicochemical properties of the samples F and H are summarized in Table 1. Sample H has a lower metal content (0.37%), a higher metal dispersion (Pd_s/Pd_t = 0.78) and consequently, a smaller average particle size (d_p = 1.4 nm).

The presence of small Pd particles on sample H was corroborated by TEM. Fig. 4a shows the presence of particles between 2 and 4 nm. Moreover, it can be noticed that particles in this size range

Table 1
Main catalysts properties.

Catalyst	Pd(%)	CO/Pd_t[a]	Pd_s/Pd_t[b]	d_p(nm)[c]
F	0.49	0.26	0.33	3.4
H	0.37	0.64	0.78	1.4

[a] From FTIR data (see text).
[b] Metal dispersion (surface Pd atoms/total Pd atoms).
[c] Particle size calculated from the metal dispersion: d_p (nm) = 1.12/(Pd_s/Pd_t).

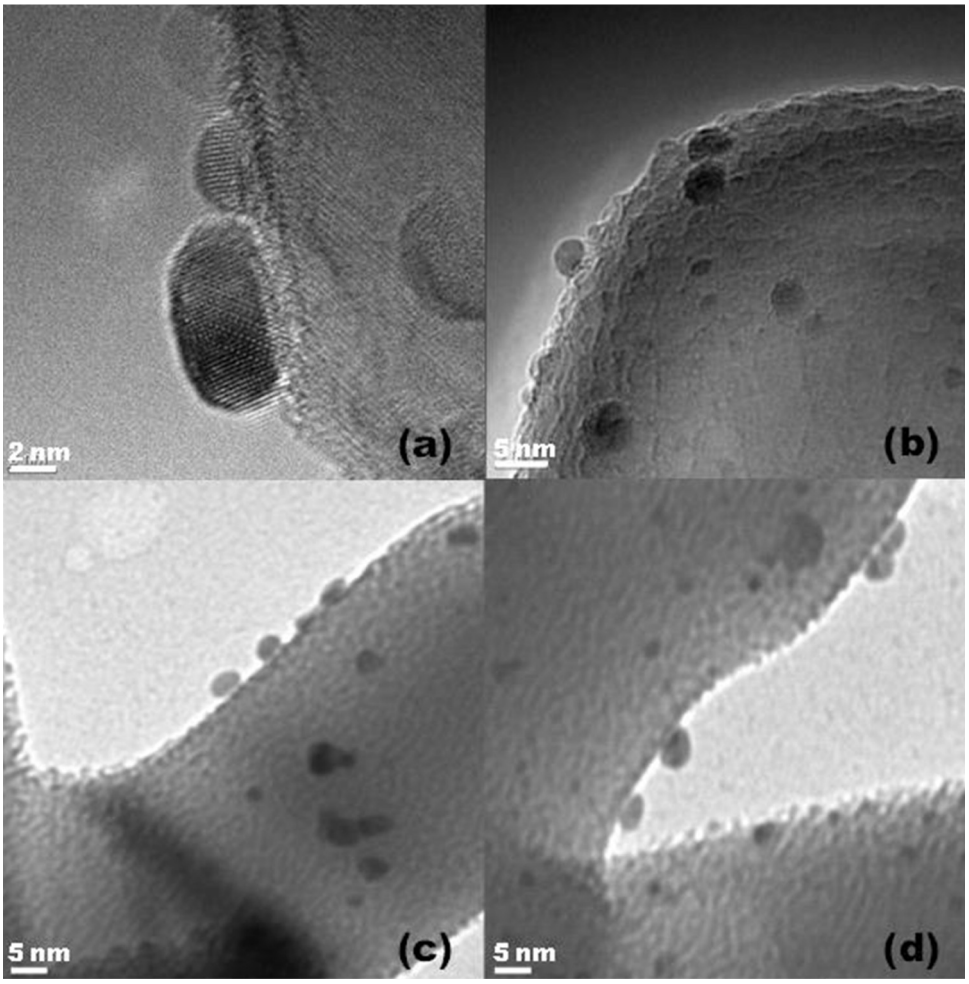

Fig. 4. TEM images of catalyst H (a and b) and catalyst F (c and d). Fresh samples.

are hemispherical in shape and they seem to be well anchored to the support material. A few particles of larger size (≅10 nm) were also observed, but with a different shape: they were quite flat with a height of 3–4 nm. The shape contrast between small and large particles is clearly seen in Fig. 4b.

These morphological features are attributed to the effect of the number of post-impregnation washing steps. On sample H, small Pd particles with a strong metal–support interaction seem to prevail after three washing steps. It was previously shown that the formation of these particles depends on the concentration of the $Pd(C_5H_7O_2)_2$ solution [12]. Based on the results of a XPS and chemisorption study, it was postulated that large particles formed under reducing conditions may be of constant height and varying diameters. The effect of successive washing steps employed in the present study seems to be equivalent to the one resulting from the use of a low concentration of the metal precursor, because non-interactive particles are removed.

Sample F was also studied by TEM analysis. Despite the lower resolution of the images it was observed that Pd particles were mainly spherical and in some cases they seem barely in contact with the support, as shown in Fig. 4c.

The hydrogen reduction profiles of the fresh samples are presented in Fig. 5. The reduction process starts at low temperature (≤0 °C), the hydrogen consumption increases continuously and peaks are located at 50 and 58 °C for samples H and F, respectively. Despite the difference in average particle size, the reduction profiles are quite similar. Asymmetric peaks are characteristic of Pd catalysts prepared by recharging [13]. The relatively high reduction temperature and the peak asymmetry may be attributed to the coexistence of Pd oxide particles of different size or shape. The profiles exhibit a negative peak with a minimum at 70–79 °C, which is due

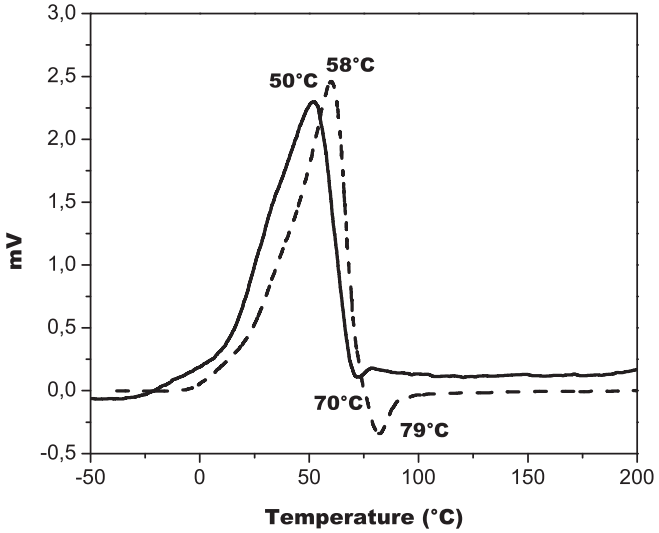

Fig. 5. Temperature programmed reduction profiles of fresh samples. Sample F (dotted line) and sample H (full line) preoxidized in air at 400 °C.

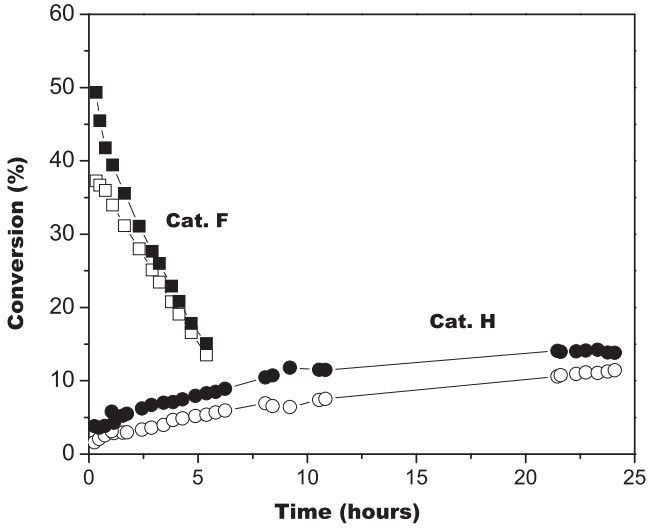

Fig. 6. CH_4 (□; ○) and CO_2 (■; ●) conversion *versus* reaction time for samples F and H. Temperature: 650 °C; feed: $CH_4/CO_2/Ar$ (25/25/50); total flow: 200 cc/min.; Cat. mass: 400 mg.

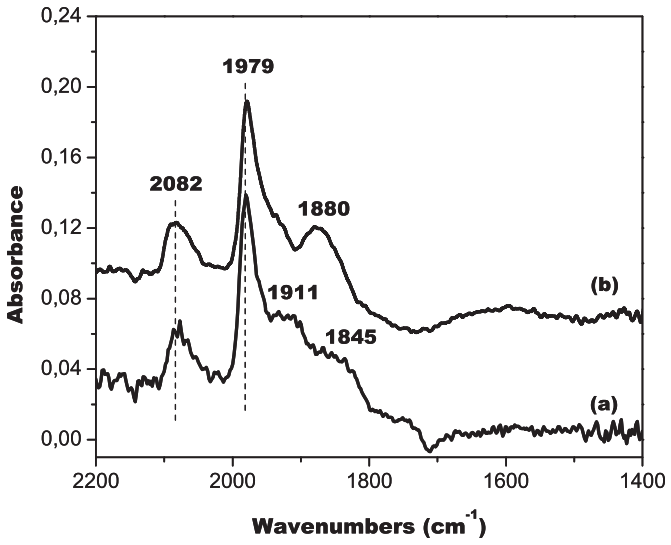

Fig. 7. FTIR spectra of used samples after an air treatment at 500 °C followed by H_2 reduction at 350 °C. Sample F (a); sample H (b).

to Pd β-hydride decomposition. This peak is more pronounced on sample F due to the larger average particle size.

When samples F and H were tested for CH_4 reforming at 650 °C, notable differences in activity were observed. As shown in Fig. 6, the F catalyst exhibits a high initial activity, followed by a marked deactivation leading to low conversion in 5 h. CO_2 conversion was initially larger than CH_4's, due to the RWGS reaction. Carbon accumulation was evidenced by the slow and continuous increase in the reactor pressure. As previously shown by HRTEM measurements, carbon formation was mainly responsible for the rapid loss in activity [7]. On a sample of similar metal loading and dispersion, fibers of 8–18 nm in diameter were observed. In contrast, sample H showed a very low initial activity that increased slowly, but continuously over a period of about 25 h reaching a steady-state value. This behavior is shown in Fig. 6.

Significant differences in selectivity were also observed. On sample F the CO/H_2 ratio remains practically constant at 1.3, in spite that the level of conversion drops considerable (from 43 to 13%) in 5 h. In addition, the CO/H_2O ratio increases from around 8–20. A decreasing production of H_2O indicated a decline of the RWGSR. This is also consistent with the similar CH_4 and CO_2 conversions observed on the deactivated sample (see Fig. 6). On the other hand during the activation of sample H the CO/H_2 ratio decreased from an initial value of 6.0–1.3 mainly due to an increasing and higher H_2 production relative to that of CO. In this case the formation of H_2O was almost constant along the run. Consequently, the activation process did not influence the RWGSR.

The previous results demonstrate that samples that exhibit a completely different activity *versus* time on stream behavior were obtained, despite the quite similar preparation conditions. Other catalysts that showed comparable results were prepared, but not fully characterized. A sample with a Pd content of 0.56 wt% and a metal dispersion of 27% (sample G), was obtained by repeating the procedure employed to prepare sample F. Another sample with a metal content of 0.11 wt% and a metal dispersion of 76% was obtained after one impregnation–washing cycle like the one employed for sample H (sample I). The CH_4 conversion of sample G declined from 55% to 8% and the conversion of sample I showed an increase from 2% to 13%, both in 24 h. In order to explain this behavior, used samples of catalysts F and H were characterized by FTIR, TPR, and TEM. Their quite similar metal content was the reason for focusing our attention on these samples.

The CO adsorption spectrum of samples F and H, obtained after a treatment in air at 500 °C to remove surface carbon followed by H_2 reduction at 350 °C were quite similar as shown in Fig. 7. On both samples the band due to linear adsorbed CO decreased in intensity and the main band was now located at 1979 cm^{-1} corresponding to CO adsorbed on the (1 0 0) plane. These changes are mainly attributed to the growth of metal particles. Only small features on the low frequency side of the spectrum are different. Sample H (spectrum (a)) presents a broad band at 1880 cm^{-1} that was not resolved on the fresh catalyst. The estimated CO/Pd ratio was 0.12 and 0.14 for samples F and H, respectively. The sintering process was more pronounced on sample H due to the longer reaction time. According to FTIR results, the surface structure of the Pd particles on both samples was similar, but the catalytic behavior was completely different. The development of the Pd (1 0 0) plane is an essential requirement for the activation of sample H.

The TPR profiles of the used samples presented in Fig. 8 showed more symmetric H_2 consumption peaks, located at lower temperatures relative to those of the fresh samples. Due to the marked growth of the metal particles on sample H, the hydrade

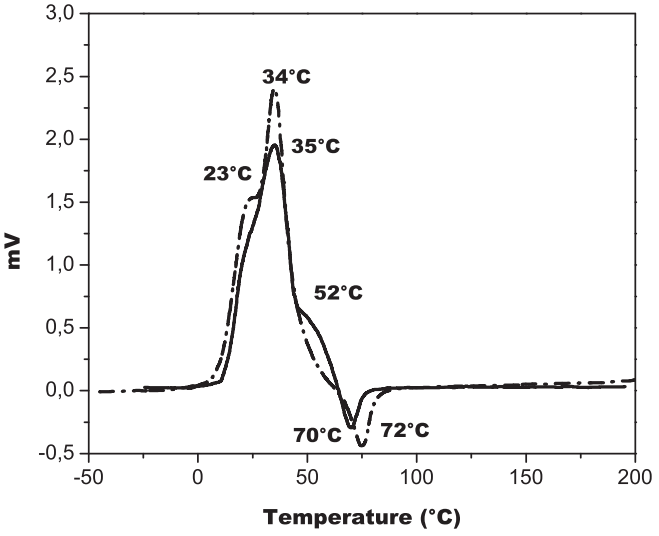

Fig. 8. Temperature programmed reduction profiles of used samples. Sample F (dotted line) and sample H (full line) preoxidized in air at 500 °C.

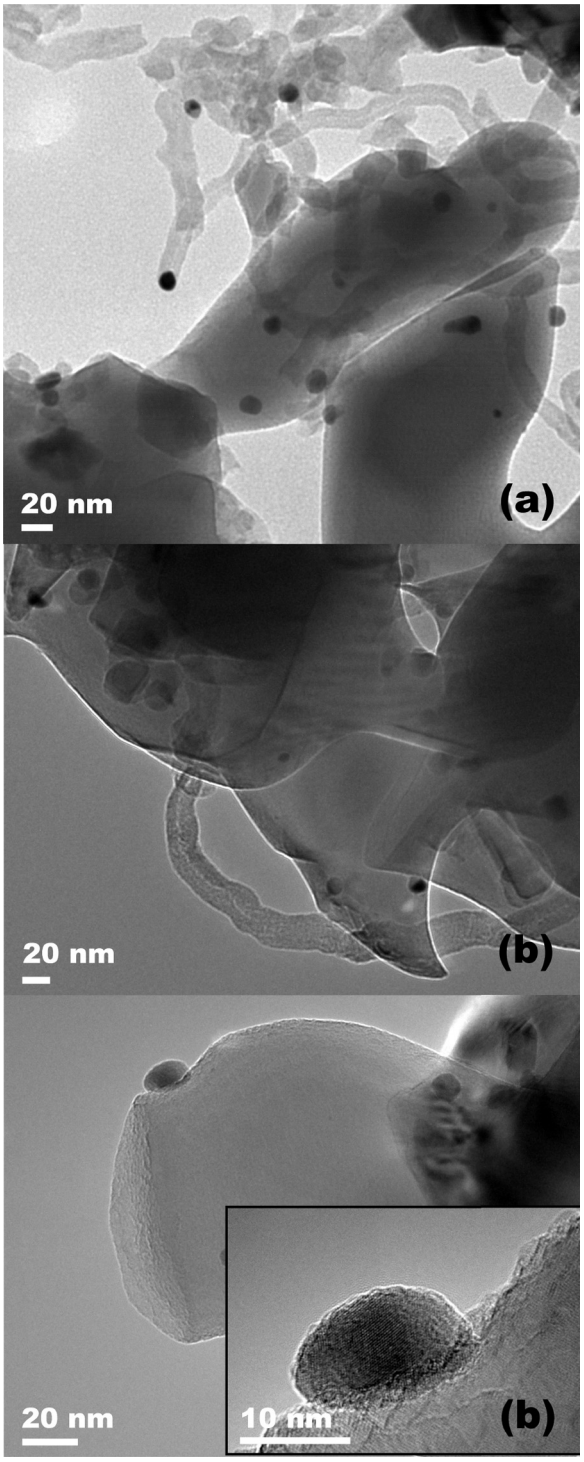

Fig. 9. TEM image of catalyst F (a) and catalyst H (b and c). Used samples.

decomposition peaks on both samples were comparable. Consequently, no significant differences in the oxidation–reduction behavior of the metal particles that could be related to the opposed catalytic behavior, were observed.

According to TEM analysis, the used samples showed particles in the 11–16 nm range that were not present on the fresh ones, which is a clear indication of sintering. However, the main difference between the F and H catalysts was on the amount of carbon nanofibers. On the F catalyst the TEM micrographs showed the abundance of loose carbon nanofibers of about 15 nm in diameter. Many fibers, but not all, showed Pd particles of spherical shape at the end. Moreover, these particles were not attached to the support as shown in Fig. 9a. Particles not associated to fibers, but anchored to the support were also observed. The TEM images of catalyst H after reaction revealed a completely different picture. Few fibers were observed, as shown in Fig. 9b. In addition, small hemispherical particles similar to those found on the fresh samples were detected, as shown in Fig. 9c.

According to the picture emerging from the TEM micrographs, the formation of carbon nanofibers depends essentially on the morphology of the metal particles, which in turn depends on the degree of interaction with the support surface. On the F catalyst, particles loosely bound to the support are easily surrounded by carbon layers derived from CH_4 decomposition. Moreover, the growth of the carbon deposits facilitates the detachment of the particle from the support surface. Consequently, CO_2 activated on the support surface or in the Pd-Al_2O_3 interface does not contribute to the elimination of carbon, enhancing the deactivation process. The behavior of catalyst F and the proposed interpretation are in line with the results of a previous study [7] performed on a Pd(0.42%)/α-Al_2O_3 without post-impregnation washing steps.

On catalyst H the use of a recharging procedure with three washing steps decreased the metal loading and increased the dispersion. The FTIR results showed that mainly Pd atoms of low coordination were exposed. On this surface the catalytic activity for CH_4 reforming with CO_2 was negligible. Under reaction conditions the growth of the metal particles by sintering was accompanied by a surface reconstruction process that favors the reforming reaction. The slow activation of the catalysts despite the decrease in surface area suggests that the carbon deposited on the Pd surface by CH_4 decomposition is being removed by reaction with CO_2. This behavior may be favored by the existence of a large Pd-Al_2O_3 boundary, resulting from the metal–support interaction, which allows the activation and/or migration of CO_2.

Although the H catalyst exhibited a continuous activation, the TEM images also showed that some Pd particles are responsible for the formation of carbon nanofibers. This result suggests that non-interactive particles or particles with a moderate interaction with the support cannot be avoided just by adjusting the impregnation–washing cycles. Consequently, detailed knowledge of the metal–support interface leading to a better control of the size and morphology of the Pd particles is required to avoid completely the growth of carbon forming particles.

4. Conclusions

Pd/α-Al_2O_3 catalysts of low metal loading (<0.5 wt %) were prepared by a recharging procedure involving 5 impregnation steps, each followed by two or three washing steps. The number of washing steps influences Pd loading, metal dispersion, surface structure and particle morphology. By using two washing steps a catalyst with a medium dispersion (33%) that exposed mainly Pd atoms on the (1 0 0) plane on approximately spherical particles was obtained.

According to TEM images, these particles seem to be weakly bound to the support surface. They exhibited a high initial activity for CH_4 reforming with CO_2 at 650 °C, followed by a pronounced deactivation due to the growth of carbon nanofibers. In this process particles were removed from the support surface. When the number of washing steps was three, a catalyst with a lower loading and a higher dispersion exposing mainly Pd atoms of low coordination was obtained. In this case, small particles were hemispherical and strongly bound to the support. Under reforming conditions they exhibited a slow activation process associated to the growth of metal particles, as revealed by TPR results.

The development of the (1 0 0) surface plane was confirmed by FTIR spectroscopy of adsorbed CO. Despite the increase in particle size, catalyst' deactivation was not observed in a 24-h long run. The TEM images revealed that particles remained bound to the support and consequently, the formation of carbon nanofibers was inhibited. These results indicate that the catalytic behavior of Pd/α-Al_2O_3 catalysts for dry reforming depends mainly on the particle morphology, which in turn is strongly influenced by the preparation conditions.

Acknowledgements

The authors wish to thank Ing. Julia Yañez (CCT, Bahía Blanca, Argentina), Dr. Prof. Christoph Somsen and Dr. Ali Aghajani (Institute for Materials, Faculty of Mechanical Engineering, Ruhr-Universität Bochum, Germany) for performing the TEM analysis.

References

[1] M.P. Kohn, M.J. Castaldi, R.J. Farrauto, Appl. Catal. B 94 (2010) 125–133.
[2] J.H. Bitter, K. Seshan, J.A. Lercher, J. Catal. 171 (1997) 279–286.
[3] A. Erdöhelyi, J. Cserényi, F. Solymosi, J. Catal. 141 (1993) 287–299.
[4] H.Y. Wang, E. Ruckenstein, Appl. Catal. A 204 (2000) 143–152.
[5] J. Wei, E. Iglesia, J. Phys. Chem. B 108 (2004) 4094–4103.
[6] P.G. Schulz, M.G. Gonzalez, C.E. Quincoces, C.E. Gigola, Ind. Eng. Chem. Res. 44 (2005) 9020–9029.
[7] M.D. Sanchez, M.S. Moreno, I. Costilla, C.E. Gigola, Catal. Today 133 (2008) 842–845.
[8] M. Ocsachoque, F. Pompeo, G. Gonzalez, Catal. Today 172 (2011) 226–231.
[9] A. Yamaguchi, E. Iglesia, J. Catal. 274 (2010) 52–63.
[10] A. Pisanu, Ph.D. thesis, Universidad Nacional del Sur, Bahia Blanca, Argentina, 1997.
[11] R. Rainer, C. Xu, D. Wayne Goodman, J. Mol. Catal. A: Chem. 119 (1997) 307–325.
[12] J. Goetz, M.A. Volpe, A.M. Sica, C.E. Gigola, R. Touroude, J. Catal. 153 (1995) 86–93.
[13] I. Costilla, Ph.D. thesis, Universidad Nacional del Sur, Bahia Blanca, Argentina, 2012 (Chapter V, Fig. 5.23).